Controlling the Morphology of Gold Films on Poly(dimethylsiloxane)

Oliver Graudejus,* Patrick Görrn, and Sigurd Wagner

Department of Electrical Engineering and Princeton Institute for the Science and Technology of Materials (PRISM), Princeton University, Princeton, New Jersey 08544

ABSTRACT Gold films on poly(dimethylsiloxane) (PDMS) have applications in stretchable electronics, tunable diffraction gratings, soft lithography and as neural interfaces. The electrical and optical properties of these films depend critically on the morphology of the gold. Therefore, we examine qualitatively and quantitatively the factors that affect the morphology of the gold film. Three morphologies can be produced controllably: microcracked, buckled, and smooth. Which morphology a gold film will adopt depends on the film stress and the growth mode of the film. The factors that affect the film stress and growth mode, and thus the morphology, are as follows: deposition temperature, film thickness, elastic modulus, adhesion layer thickness, surface properties of the PDMS, and mechanical prestrain applied during deposition. We discuss how the different components of the film stress and growth mode of the film affect the morphology.

KEYWORDS: flexible electronics • gold • thin films • stress • elastomers

INTRODUCTION

Gold films on poly(dimethylsiloxane) (PDMS) enable stretchable electronic applications such as dielectric elastomer actuators (DEAs) (1), sensitive electronic skin (2, 3), stretchable interconnects (4, 5), and microelectrodes for neural interfaces in biomedical engineering (6–8). Other applications for gold films on PDMS are tunable diffraction gratings (9), physical self assembly to pattern stamps for soft lithography (10, 11), and nanotransfer printing (nTP) (12). Gold films on PDMS can assume three different morphologies: microcracked, buckled, or smooth. Their electrical conduction and optical reflectance depend profoundly on this morphology. Table 1 summarizes the visual appearance, optical micrographs and secondary electron micrographs (SEMs), and appropriate applications for each morphology.

Microcracked and buckled gold films are of particular interest for stretchable electronics because they remain electrically conducting when stretched (5, 13, 14). Buckled films require a mechanical prestrain of the PDMS substrate during gold deposition to remain electrically conducting beyond ∼5% strain (15). They remain electrically conducting until stretched flat when stretched in the direction perpendicular to the buckles. The larger the mechanical prestrain, which increases the amplitude of the buckles once relaxed (16), the more the samples can be stretched until they are flat. Microcracked films remain electrically conducting beyond 50% strain (13) and offer a combination of desirable properties for the fabrication of stretchable electronics. These properties are (1) low electrical resistance, (2) compatibility with standard microfabrication technology without the requirement for mechanical prestrain, (3) higher accuracy of lithographic patterning than that of buckled films because microcracked films are nearly flat, (4) negligible effect of the gold film on the elastic modulus of the Au/PDMS composite, and (5) low fatigue, with a proven capability of isotropically stretching and relaxing for at least 250 000 cycles (17).

Controlling the morphology is very important for commercial applications of stretchable electronics because the properties of the gold film profoundly depend on the morphology. To control the morphology effectively requires a qualitative and quantitative knowledge of the process parameters that affect the morphology. While Bowden et al. (10) demonstrated that high sample temperatures during gold deposition are required to obtain buckled gold films on PDMS that is not mechanically prestrained, the process parameters for microfabrication of microcracked films have not yet been defined. Therefore, we evaluated qualitatively and quantitatively the conditions that produce microcracked gold films. We also identify the relative importance of externally applied mechanical, thermal, and intrinsic stresses, all of which affect the morphology.

EXPERIMENTAL SECTION

Preparation of PDMS Membranes. The silicone prepolymer and the cross linker were mixed in a 10:1 ratio by weight (PDMS; Sylgard®184 from Dow Corning), degassed in vacuum, and spun on a glass slide at 250 rpm for 50 s. The PDMS was cured at three different temperatures: (i) 60 °C for at least 24 h, (ii) 95 °C for 45 min, and (iii) room temperature for at least 2 days. This preparation produced a 300-μm-thick elastomeric silicone membrane. Curing procedures (i) and (ii) produced PDMS substrates with an elastic modulus $E_{sub} = 2$ MPa; procedure (iii) made $E_{sub} = 1$ MPa.

Measurement of the Elastic Modulus. The elastic moduli E_{sub} of PDMS samples were obtained from stress−strain measure-
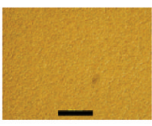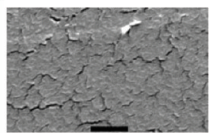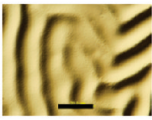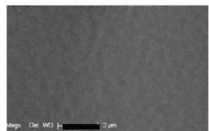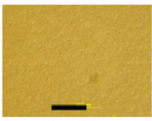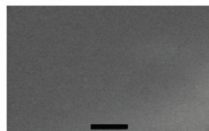
Table 1. Morphologies of Gold Films on PDMS and Their Applications[a]

morphology	visual appearance	optical microscope	SEM	application
microcracked	reflective, gold color			stretchable interconnect, microelectrodes
buckled λ=10-50μm	frosted gold or yellow-white color			physical self assembly, tunable diffraction gratings, stretchable interconnects
smooth	reflective, gold or blue color			DEAs, nTP

[a] The scale bar for optical micrographs is 20 μm and that for SEM images 2 μm.

ments with an Instron 5865 extensometer. The elastic modulus is the slope of the stress—strain plot in the linear region (strain <10%).

Metal Deposition. The metal stack of 30 Å of chromium or titanium, followed by 30—2500 Å of gold, was deposited by electron-beam evaporation (DV-502A, Denton). The deposition rate was 4—8 Å/s. The samples were rotated during deposition. A quartz crystal monitor was used to measure the film thickness.

Patterning. The gold film was patterned by conventional photolithography and etching. The photoresist (AZ5214, Clariant) was spun on the gold-coated PDMS, followed by exposure (MJB3, Karl Suss) through a photomask and development (AZ312MIF, Clariant). Etching the exposed gold film with a GE6 solution (KI, I_2 in H_2O, Transene) transferred the mask pattern onto the film. The resist was then stripped by UV exposure and soaking in the developer (AZ312MIF).

Temperature Measurement. The deposition temperature during evaporation was measured with a thermocouple (TC) located next to the rotating sample holder, allowing convenient reading of the nominal temperature during metal deposition. However, this nominal temperature does not equal the sample temperature because (i) the TC was mounted >5 cm away from the location of the sample and (ii) the thermal masses of the TC and PDMS were different. To correlate the nominal deposition temperature more closely with the actual sample temperature, we measured the deposition temperature at the sample location on the sample holder with a chromel—alumel (type K), low-thermal-mass TC (see the Supporting Information for details). We use the calibrated T_{dep} throughout this article to describe the temperature during deposition because this temperature is closer to the real temperature of the sample during deposition.

Prestrained Samples. Samples with varying mechanical prestrain were obtained by bending a PDMS/polyimide (PI) stack to a parabola. The 50-μm-thick PI carrier foils were 50 mm long and 25 mm wide. Before the PMDS was spun on, the PI foil was made to adhere to a glass slide with several drops of water. After curing, the PDMS/PI stack was bent parabolically such that the distance between the two ends was 38 mm and the maximum deflection in the center was 12 mm.

Plasma Oxidation. The PDMS surface was plasma-oxidized in a Plasma-Therm 790 reactive ion etcher.

SEM Images. SEM images were taken with an FEI XL30 equipped with a field-emission gun.

Atomic Force Microscopy Images. The amplitude of the buckles was measured using a DI Nanoscope IIIa atomic force microscope in tapping mode, tips with a force constant of $k = 3$ N/m.

RESULTS

We observed three types of morphologies for the gold films on 300-μm-thick PDMS:

(1) Microcracked films have 0.5—2-μm-long cracks and a typical gold-colored appearance to the unarmed eye. The microcracks form during gold deposition.

(2) Buckled films have waves with wavelengths of 10—50 μm. These films have a frosted gold color for amplitudes >1.5 μm and are nearly white for amplitudes <1 μm.

(3) Smooth gold films are characterized by the absence of microcracks or buckles. These films are nearly flat and appear similar to a gold film on glass. The gold film is discontinuous if the gold thickness is less than about 160 Å. When the sample lies on a white surface and is viewed from the top, it has the typical gold color when the film is thicker than ~60 Å and appears blue when thinner. Such films are electrically conducting at a thickness larger than ~50—60 Å.

We carried out several experiments to elucidate the mechanism of microcrack formation because this is the morphology important to our device (14).

Deposition Temperature, T_{dep}, and Film Thickness, d_{Au}. In Figure 1, the temperature at the end of deposition, T_{dep}, is plotted versus the thickness of the gold film, d_{Au}, for PDMS with $E_{sub} = 1$ MPa (Figure 1a) and 2 MPa (Figure 1b). It is seen that the morphology of the gold film strongly depends on T_{dep} and d_{Au}. Gold films are microc-racked for $d_{Au} \sim 180—1300$ Å and $T_{dep} < 60—65$ °C. The gold film is smooth for $d_{Au} \sim 160—450$ Å if T_{dep} is >60—65 °C and is discontinuous for $d_{Au} < 160$ Å regardless of T_{dep}. The gold film is buckled for $d_{Au} > 450—500$ Å and T_{dep}
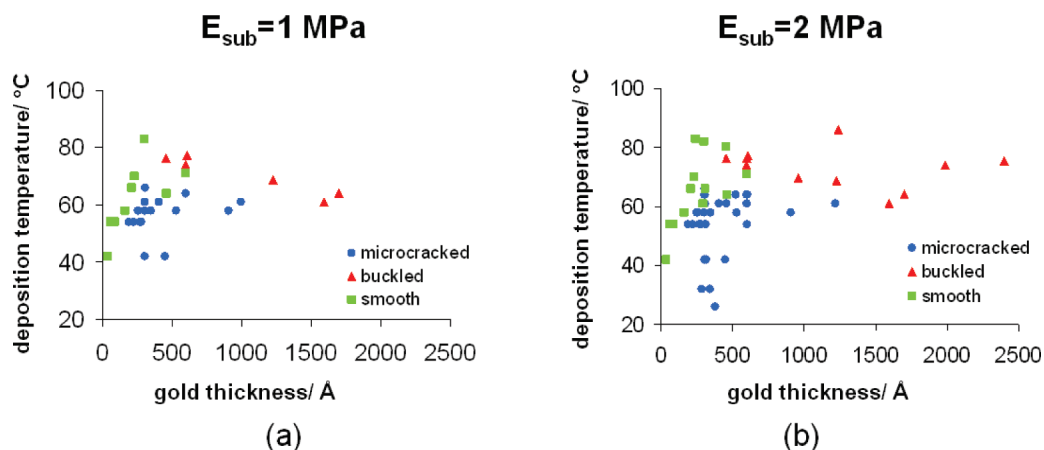
E_{sub}=1 MPa

E_{sub}=2 MPa

(a)

(b)

FIGURE 1. Morphology of gold films for ranges of film thickness and deposition temperature on PDMS substrates with elastic moduli E_{sub} of (a) 1 MPa and (b) 2 MPa.
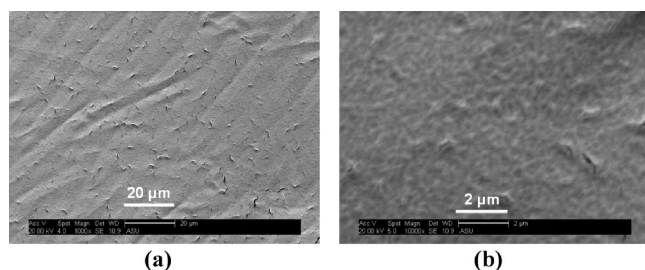

(a)   (b)

FIGURE 2. SEM micrograph of a gold film on PDMS after sequential deposition of 30 Å of chromium and seven 300-Å-thick layers of gold (for a total gold thickness of 2100 Å). The time between each layer deposition was at least 30 min. Magnification: (a) 1000 times; (b) 10 000 times.

> 60−80 °C. The minimum d_{Au} for buckling is 450−500 Å. No buckling is observed regardless of T_{dep} for d_{Au} < 450 Å. The minimum T_{dep} required to cause the film to buckle generally decreases with increasing d_{Au}. For example, a 1600-Å-thick film buckles at T_{dep} = 60 °C, whereas a 600-Å-thick film requires T_{dep} = 75 °C to buckle. For d_{Au} > 2000 Å, the film always buckles, regardless of T_{dep}.

Elastic Modulus. There is little difference between parts a (E_{sub} = 1 MPa) and b (E_{sub} = 2 MPa) of Figure 1; i.e., no appreciable effect of the elastic modulus on the morphology of the film was observed for E_{sub} between 1 and 2 MPa.

Sequential Deposition. Figure 2 shows the SEM micrograph of a sequential deposition of 30 Å of chromium followed by seven 300 Å depositions of gold (for a total of 2100 Å) on 300-μm-thick PDMS. The time between depositions was 30 min, allowing the sample to cool to room temperature between depositions. The SEM micrographs show that the gold film is buckled with a small density of microcracks. Gold films deposited in the same manner (i) on 80-μm-thick PDMS (spun on at 1000 rpm) or (ii) with four depositions of 500 Å on 300-μm-thick PDMS gave SEM micrographs similar to those shown in Figure 2.

Evaporation Through a Shadow Mask. Figure 3 shows the SEM micrograph of a 3000-Å-thick gold film deposited on PDMS through a 2 × 2 mm² shadow mask. A buckled center region connects to a "frame" of large and small cracks that extends 200−300 μm from the edge of the shadow mask.

Etching a Buckled Film. Figure 4 shows a gold film with random buckles before (Figure 4a) and after (Figure 4b) etching. The PDMS remains buckled in those areas on the sample where the gold film was etched.

Adhesion Layer Thickness, $d_{adhesion}$. Chromium adhesion layers of 0, 30, 60, 90, and 110 Å thickness followed by 300 Å of gold were deposited on PMDS (E_{sub} = 2 MPa). Figure 5 shows the SEM images of the resulting films. For 0, 30, and 60 Å chromium thickness, the film is microcracked. For 90 and 110 Å chromium thickness, the film is smooth. Gold films of 300 Å thickness with an even thicker $d_{adhesion}$ layer are buckled with a wavelength of ~1 μm.

Plasma-Treated PDMS. PDMS was treated with an oxygen plasma before metal deposition. An adhesion layer of 30 Å chromium or titanium was evaporated first, followed by gold deposition. Various deposition temperatures and gold thicknesses were investigated. These gold films are always smooth or buckled, depending on the deposition conditions, but never microcracked, even for mild and brief plasma treatments (power density, 20 mW/cm²; pressure, 100 mTorr; O_2 flow, 10 sccm; Ar flow, 40 sccm; exposure time, 5 s).

Mechanical Prestrain. The mechanical prestrain $\varepsilon_{mech,pre}$ was applied to the substrate (E_{sub} = 2 MPa) prior to deposition by bending a 250-μm-thick PDMS membrane lined to a 50-μm-thick PI foil (E_{PI} = 5 GPa) to a parabola. $\varepsilon_{mech,pre}$ on the PDMS surface is a function of its local radius of curvature. The radius of curvature decreases from the ends to the center of the parabola; hence, the prestrain increases in the same direction:

$$\varepsilon_{mech,pre} = \frac{\text{distance from the neutral plane}}{\text{radius of curvature}} \approx \frac{\text{PDMS thickness} + 0.5(\text{PI thickness})}{\text{radius of curvature}} \quad (1)$$

The neutral plane is near the center of the PI foil because the elastic modulus of the PI foil is much larger than of that of PDMS. Thus, the distance of the PDMS surface from the
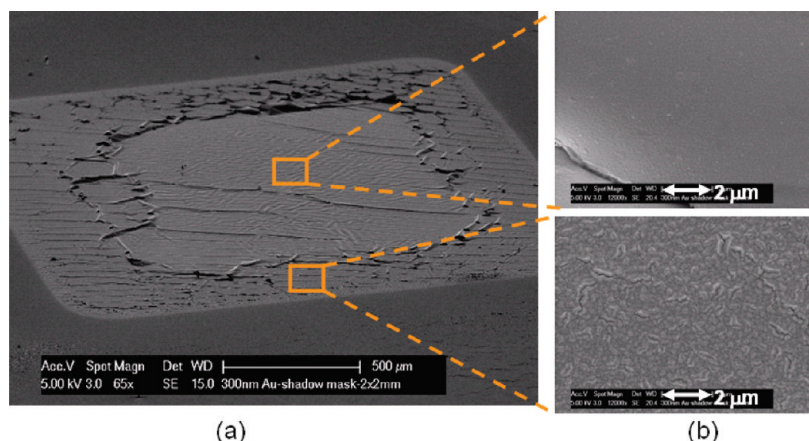
FIGURE 3. (a) SEM micrograph of a 2 × 2 mm² wide, 3000-Å-thick gold pad on PMDS deposited through a shadow mask and (b) details from the center and the edge regions.
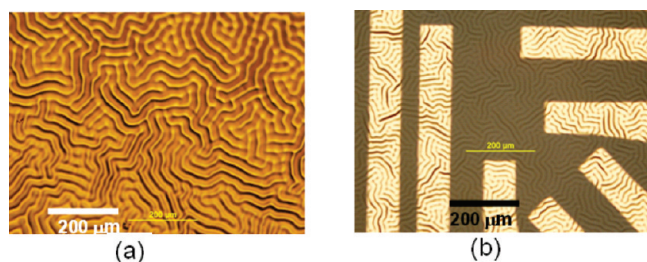

FIGURE 4. Random wrinkles of a gold film (a) on PDMS and (b) after partial removal of the gold film by wet etching. Note that the exposed PDMS surface (dark) retains the wrinkle pattern.

neutral plane equals the thickness of PDMS plus half the thickness of the PI foil. Figure 6a shows the calculated $\varepsilon_{\text{mech,pre}}$ for a 50-mm-long PDMS/PI stack with a parabolic bend.

A 350-Å-thick gold film ($T_{\text{dep}} \sim 32$ °C) was deposited simultaneously on mechanically prestrained PDMS and on a flat, relaxed PDMS substrate on a glass carrier. Both samples had microcracks and the typical reflective gold color, except for a region that covered ∼5 mm to both sides of the center of the prestrained sample, corresponding to $\varepsilon_{\text{mech,pre}} > 1.7\%$ (see Figure 6b). Variations of d_{Au} due to the bend of the parabola are <8 % and can therefore not account for the observed change in morphology. A mechanical prestrain of ∼1.7 % appears to be a threshold in that higher values cause the film to buckle and lower values produce the same morphology as that on the relaxed control sample.

DISCUSSION

Whether gold films with a microcracked, buckled, or smooth morphology form on PDMS depends on the compressive and tensile stresses in the film. We illustrate the formation of these morphologies by analyzing the individual stress components in the film. The total stress σ_{tot} in the film equals the sum of the following components:

$$\sigma_{\text{tot}} = \sigma_{\text{th,pre}} + \sigma_{\text{th,dep}} + \sigma_{\text{int}} + \sigma_{\text{mech,pre}} \qquad (2)$$

$\sigma_{\text{th,pre}}$ and $\sigma_{\text{th,dep}}$ are the thermal stresses (σ_{th}) in the film caused by the large mismatch in the coefficients of thermal

expansion (CTE) between PDMS ($\text{CTE}_{\text{PDMS}} = 300 \times 10^{-6}\,\text{K}^{-1}$) and gold ($\text{CTE}_{\text{Au}} = 14.4 \times 10^{-6}\,\text{K}^{-1}$). $\sigma_{\text{th,pre}}$ is the thermal stress caused by the heating of PDMS before deposition, i.e., during the heatup of the evaporating metal with the substrate shutter closed. $\sigma_{\text{th,dep}}$ is the thermal stress caused by the heating of PDMS during gold deposition with the substrate shutter being open. The heating of PDMS is mainly caused by dissipation of the kinetic energy of the impinging metal atoms, their heat of condensation, and the radiation energy of the glowing metal. σ_{int} is the intrinsic stress that is inherent to the growing film and therefore depends on the growth mode of the film. $\sigma_{\text{mech,pre}}$ is the stress in the film that is caused by an externally applied mechanical prestrain in PDMS during metal deposition. $\sigma_{\text{mech,pre}} = 0$ Pa if no prestrain is applied.

$\sigma_{\text{mech,pre}}$ and $\sigma_{\text{th,pre}}$ always result in compressive stress in the film. Both of these stress components cause PDMS to be under tensile stress at the beginning of the deposition, either due to mechanical force ($\sigma_{\text{mech,pre}}$) or due to thermal expansion ($\sigma_{\text{th,pre}}$). Release of this tensile stress after deposition, by relaxation of the prestrain ($\sigma_{\text{mech,pre}}$) or cooldown to room temperature ($\sigma_{\text{th,pre}}$), respectively, causes a compressive stress in the gold film. $\sigma_{\text{th,dep}}$ causes a tensile stress in the growing film during deposition as T_{dep} continues to rise, which is followed by compression during cooldown. σ_{int} can be either compressive or tensile, depending on d_{Au}. Gold films follow a Volmer−Weber growth mode when deposited on surfaces that allow high adatom mobility (low adatom−surface interaction), such as MgF$_2$ (18) and silicon nitride (19). Because PDMS has a low surface energy of 0.02 J/m (20), gold films on PDMS likely follow the Volmer−Weber growth mode. Further evidence that gold films on PDMS may behave similarly as on MgF$_2$ and silicon nitride is provided by the fact that the thickness at which the film becomes electrically conducting is about 60 Å on all of these substrates. In Volmer−Weber growth, the main sources of σ_{int} are grain growth and grain-boundary growth during island coalescence. On MgF$_2$, gold films have a maximum intrinsic tensile stress of ∼90 MPa at $d_{\text{Au}} \sim 160$ Å (18), where island coalescence is complete. For thicker films, the intrinsic tensile stress decreases and disappears at $d_{\text{Au}} \sim 230$ Å.
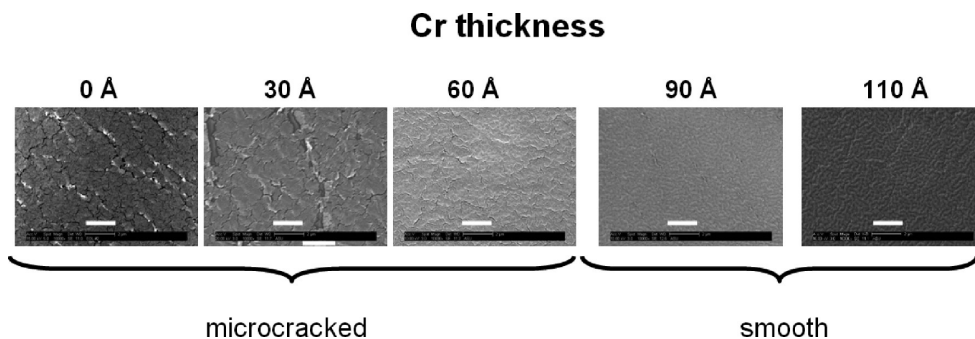
Cr thickness

FIGURE 5. Morphology of a gold film ($d_{Au} = 300$ Å) for different chromium adhesion layer thicknesses. The film is microcracked for $d_{Cr} = 0$, 30, and 60 Å and is smooth for $d_{Cr} = 90$ and 110 Å. Scale bar: 2μm.
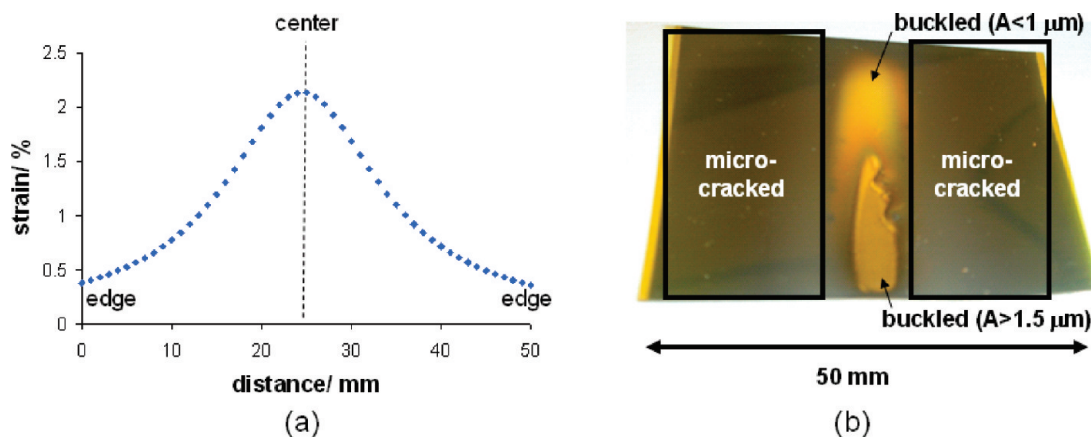

FIGURE 6. (a) Tensile mechanical prestrain of parabolically bent PDMS versus location and (b) gold film deposited on mechanically prestrained PDMS using process conditions that result in microcracked films on glass-backed PDMS (A = buckle amplitude).

Even thicker films show a compressive stress. The numbers are similar for gold films on silicon nitride.

The gold film is buckled if σ_{tot} is compressive and exceeds the critical stress for buckling, σ_{crit}. Buckling relieves the stress in the film by the formation of sinusoidal wave patterns. σ_{crit} depends on the mechanical properties of the film and substrate. σ_{crit} equals (10)

$$\sigma_{crit} \approx 0.52 \left(\frac{E_m}{1 - v_m^2} \right)^{1/3} \left(\frac{E_{sub}}{1 - v_{sub}^2} \right)^{2/3} \quad (3)$$

where m stands for metal, sub for substrate, and v for Poisson ratio. According to eq 3, σ_{crit} of a gold film ($E_m = 78$ GPa and $v_m = 0.33$) on as-fabricated PDMS ($E_{sub} = 2$ MPa and $v_{sub} = 0.5$) equals 44 MPa; i.e., the gold buckles if the compressive stress in the film exceeds 44 MPa, which corresponds to a strain of <0.1 %. Gold films are microcracked if the tensile stress in the growing film exceeds a critical value and are smooth if neither the compressive nor tensile stress in the film is large enough to cause buckling or microcrack formation, respectively.

Another factor that affects the morphology of the film is its growth mode. A pronounced three-dimensional island growth (Volmer–Weber mode) favors the formation of microcracked films, whereas a two-dimensional layer-by-layer growth (Frank–Van der Merwe mode) favors the formation of a film with smooth surfaces that might buckle during cooldown.

The stress and growth mode in gold films on PDMS are a complex function of the following parameters: gold thickness, d_{Au}; deposition temperature, T_{dep}; elastic modulus of PDMS, E_{sub}; adhesion layer thickness, $d_{adhesion}$; surface properties of PDMS (O_2 plasma treatment); mechanical prestrain of PDMS, $\sigma_{mech,pre}$.

Now, we proceed to describe the effect of each of these factors on the appearance of each morphology, with a focus on microcracked films.

Deposition Temperature, T_{dep}, and Gold Thickness, d_{Au}. As shown in Figure 1, the morphology of the film on as-prepared PDMS is a strong function of T_{dep} (causing σ_{th}) and d_{Au} (causing σ_{int}). To obtain microcracked films, T_{dep} must be kept below 60–65 °C. Thus, unavoidable heating of PDMS before the beginning of deposition (i.e., during heatup of the crucible with gold) must be kept to a minimum. The tensile stress required for microcrack formation has thermal and intrinsic components. The thermal component from expansion of PDMS dominates for thicker films, where the instrinsic stress is compressive. The intrinsic component from island coalescence dominates for thin films, where σ_{th} is low. It may therefore be no coincidence that the lowest d_{Au} at which we observed microcracks (~180 Å) nearly coincides with the thickness of 160 Å for the maximum intrinsic tensile stress observed on MgF_2 substrates (18).

It is generally difficult to obtain microcracked films with $d_{Au} > 1300$ Å. These films are buckled for any examined

temperature because $\sigma_{\text{tot}} > \sigma_{\text{crit}}$. To investigate whether the internal or thermal stress is the major component of σ_{tot}, we carried out two experiments: (1) Sequential deposition of seven 300-Å-thick layers of gold, allowing 30 min of cooldown between layer depositions. The gold film is buckled even though the temperature of PDMS is kept low. The film also has a low density of microcracks. (2) Deposition of 3000 Å of gold through a shadow mask. The gold film is buckled at the center of the square ($\sigma_{\text{tot}} > \sigma_{\text{crit}}$). The gold film also has a low density of microcracks within $200-300$ μm of the edge of the mask, similar to the film after sequential deposition. The shadow mask prevents underlying PDMS from heating up because it blocks gold atoms and radiation. Because of heat transfer, T_{dep} is lower near the edge of the exposed square than in the center (lower thermal stress). We conclude from these experiments that, at $d_{\text{Au}} > 2000$ Å, typical microcracked films are not obtained because the compressive internal stress in the thick gold film is large. If T_{dep} is kept low, microcracks with a much smaller crack density than is typical can be obtained.

On relaxed PDMS substrates, gold films adopt a buckled morphology if $d_{\text{Au}} > 450-500$ Å and $T_{\text{dep}} > 60-65$ °C. The film buckles if

$$\sigma_{\text{th,pre}} + \sigma_{\text{th,dep}} + \sigma_{\text{int}} > \sigma_{\text{crit}} \qquad (4)$$

a condition that agrees with the observation in Figure 1 that the minimum T_{dep} required to cause buckling decreases with increasing d_{Au}. The reason for this behavior is that σ_{int} becomes more compressive as d_{Au} increases (18), which means that the required thermal stress for buckling (i.e., $\sigma_{\text{crit}} - \sigma_{\text{int}}$) decreases. If d_{Au} is <450 Å, the film never buckles within the examined temperature range, indicating that the total compressive stress in this thickness range is always <σ_{crit}. The fact that the PDMS surface retains the buckled structure after the gold film is etched away (Figure 4) indicates that the PDMS surface was altered during deposition (21).

Gold films are smooth if $d_{\text{Au}} \sim 160-450$ Å at $T_{\text{dep}} > 60-65$ °C. The observation that for a given d_{Au} (i.e., constant σ_{int}) a low T_{dep} causes microcracks whereas a higher T_{dep} causes neither microcracks nor buckling is counterintuitive at first. We surmise that the higher the temperature at the beginning of deposition, the smaller the lateral expansion, i.e., the smaller the thermally induced tensile stress, during deposition. Microcracks do not form if the temperature at the beginning of the deposition is high because the tensile stress during deposition is low. An alternative explanation is that the growth mode of the film changes from a low-mobility Volmer−Weber mode at low T_{dep} to a high-mobility Volmer−Weber mode at high T_{dep} (22). The morphology of the gold film might also be affected by the increased surface diffusion of gold as T_{dep} rises, which will accelerate the recrystallization and elimination of grain boundaries (23).

Elastic Modulus of PDMS, E_{sub}. We examined the effect of the curing temperature of PDMS on the morphology of the gold films. We investigated the commercially available Sylgard®184 because it is used often by research groups working on applications that require gold films on silicone substrates (1−10). The elastic modulus of PDMS did not have an appreciable effect on the morphology of the gold film for E_{sub} between 1 and 2 MPa; i.e., the morphology of the film is not dependent on the elastic modulus within the examined range. However, because σ_{crit} is a function of E_{sub} (eq 3), the plot in Figure 1 will look different for much stiffer substrates.

Adhesion Layer Thickness, d_{adhesion}. Chromium and titanium are both good adhesion layers for gold films on PDMS. Chromium is often preferred for electronic applications because it can be sputtered and thermally evaporated, whereas electron-beam-evaporated titanium is preferred for its biocompatibility in biomedical applications. We find no difference in gold morphologies between chromium or titanium adhesion layers of the same thickness. The gold films are microcracked for $d_{\text{adhesion}} < 60$ Å and smooth for $d_{\text{adhesion}} = 90$ and 110 Å. We interpret this observation as a change in the growth mode of the gold film from largely Volmer−Weber to largely Frank−Van der Merwe (24), a change induced by the transition from low to high surface coverage by the adhesion layer (25).

Surface Properties of PDMS (O_2 Plasma Treatment). In microfluidics and stretchable electronics applications, plasma treatment of the PDMS surface is often used to increase the surface energy, thereby improving adhesion to glass, other PDMS membranes, and metal films (26). The titanium or chromium/gold film stack does indeed adhere much better to plasma-treated rather than as-prepared PDMS surfaces. However, the film never has the microcracked morphology, regardless of T_{dep}, that is required for superior stretchability. The film is either smooth or buckled, depending on T_{dep} and d_{Au}. The adhesion of the film to the elastomeric substrate must be controlled carefully. If the adhesion is poor, the metal film delaminates during lithographic patterning, and if the adhesion is too strong, microcracks do not form. The reason for this behavior may be a change in the growth mode of the film. Titanium or chromium deposited on plasma-treated PDMS follows a growth mode that more closely resembles a Frank−Van der Merwe mode than that deposited on as-prepared PDMS (23). This change in the growth mode on plasma-treated PDMS occurs because chromium and titanium are electropositive metals and are therefore less mobile on oxidized surfaces (activated PDMS or SiO_2) than on as-prepared PDMS. Thus, depositing a gold film (i) with a thin adhesion layer (10−50 Å titanium or chromium) on activated PDMS or (ii) with a thick (>100 Å) adhesion layer on as-prepared PDMS both alter the growth mode from Volmer−Weber toward Frank−Van der Merwe.

Microcracked gold films are only obtained on plasma-treated PDMS (and on SiO_2) when $d_{\text{adhesion}} = 0$ Å (26, 12). The difference in behavior of gold films on plasma-treated PDMS with and without an adhesion layer may also be due to a change in the growth mode of the film. Gold is a noble metal and therefore not as easily oxidized as titanium or

Table 2. Summary of the Process Conditions Required for the Formation of Microcracked, Buckled, and Smooth Gold Films on PDMS[a]

morphology	deposition temp (°C)	gold thickness (Å)	elastic modulus of PDMS (MPa)	adhesion layer thickness (Å)	plasma-treated PDMS	mechanical prestrain (%)
microcracked	<60−65	>180	1 or 2	<60	only without an adhesion layer	<1.7
buckled	>60−65	>450	1 or 2	any	observed	>1.7
smooth	>60−65	160−450	1 or 2	any	observed	not observed (low T_{dep})

[a] Gold films thinner than ∼160 Å are discontinuous.

chromium. It therefore retains high mobility even on oxidized surfaces, leading to Volmer−Weber growth.

Mechanical Prestrain of PDMS, $\sigma_{mech,pre}$. Buckled films with $d_{Au} < 450$ Å can only be obtained on mechanically prestrained PDMS. According to eq 2, the thermal and internal stress required for a given σ_{tot} is lower if a mechanical prestrain is applied. For example, a 350-Å-thick film buckles if $\varepsilon_{mech,pre} > 1.7\%$ even though the thermal stress is very low ($T_{dep} \sim 32$ °C). The film is microcracked if $\varepsilon_{mech,pre} < 1.7\%$. $\varepsilon_{mech,pre}$ required for the compressive stress to exceed σ_{crit} is much higher than the <0.1 % strain calculated according to eq 3. One reason for this behavior is that E_{sub} at the surface of PDMS is increased by the deposition process by additional cross-linking and possibly in-diffusion of gold (10). Schmid et al. have reported that a 30 s exposure of PDMS to the radiation emitted from a source that was heated with an electron beam induces cross-linking at the PDMS surface. The cross-linking causes sufficient hardening of the surface for wrinkles to form under compression (21).

Table 2 summarizes the process conditions required to obtain a given morphology.

CONCLUSION

Gold films on PDMS can adopt three morphologies: microcracked, buckled, and smooth. The morphology depends mainly on six factors: the gold thickness, deposition temperature, elastic modulus of PDMS, adhesion layer thickness, surface properties of PDMS (O_2 plasma treatment), and mechanical prestrain of PDMS. The findings reported in this article describe the effect of each of these factors on the morphology of the gold film. The work we report here will help to accelerate the introduction of this fascinating new technology.

Supporting Information Available: Calibration data used to correlate the nominal and actual T_{dep}. This material is available free of charge via the Internet at http://pubs.acs.org.

REFERENCES AND NOTES

(1) Pelrine, R.; Kornbluh, R.; Kofod, G. *Adv. Mater.* **2000**, *12* (16), 1223.
(2) Wagner, S.; Lacour, S. P.; Jones, J.; Hsu, P. I.; Sturm, J. C.; Li, T.; Suo, Z. *Physica E* **2004**, *25*, 326.
(3) Cotton, D. P. J.; Graz, I. M.; Lacour, S. P. *IEEE Sens. J.* **2009**, *9* (12), 2008.
(4) Carta, R.; Jourand, P.; Hermans, B.; Thoné, J.; Brosteaux, D.; Vervust, T.; Bossuyt, F.; Axisa, F.; Vanfleteren, J.; Puers, R. *Sens. Actuators, A* **2009**, *156*, 79.
(5) Lacour, S. P.; Jones, J.; Wagner, S.; Li, T.; Suo, Z. *Proc. IEEE* **2005**, *93* (8), 1459.
(6) Yu, Z.; Graudejus, O.; Tsay, C.; Lacour, S. P.; Wagner, S.; Morrison, B. *J. Neurotraum.* **2009**, *26* (7), 1135.
(7) Meacham, K. W.; Giuly, R. J.; Guo, L.; Hochman, S.; DeWeerth, S. P. *Biomed. Microdevices* **2008**, *10* (2), 259.
(8) Fitzgerald, J. J.; Lacour, S. P.; McMaho, S. B.; Fawcett, J. W. *IEEE Trans. Biomed. Eng.* **2009**, *56* (5), 1524.
(9) Yu, C.; O'Brien, K.; Zhang, Y. H.; Yu, H.; Jiang, H. *Appl. Phys. Lett.* **2010**, *96*, 041111.
(10) Bowden, N.; Brittain, S.; Evans, A. G.; Hutchinson, J. W.; Whitesides, G. M. *Nature* **1998**, *393*, 146.
(11) Huck, W. T. S.; Bowden, N.; Onck, P.; Pardoen, T.; Hutchinson, J. W.; Whitesides, G. M. *Langmuir* **2000**, *16*, 3497.
(12) Menard, E.; Bilhaut, L.; Zaumseil, J.; Rogers, J. A. *Langmuir* **2004**, *20*, 6871.
(13) Lacour, S. P.; Chan, D.; Wagner, S.; Li, T.; Suo, Z. *Appl. Phys. Lett.* **2006**, *88*, 204103.
(14) Graudejus, O.; Yu, Z.; Jones, J.; Morrison, B., III; Wagner, S. *J. Electrochem. Soc.* **2009**, *156* (6), P85.
(15) Jones, J.; Lacour, S. P.; Wagner, S.; Suo, Z. *J. Vac. Sci. Technol. A* **2004**, *22* (4), 1723.
(16) Khang, D. Y.; Rogers, J. A.; Lee, H. H. *Adv. Funct. Mater.* **2008**, *18*, 1.
(17) Graz, I. M.; Cotton, D. P. J.; Lacour, S. P. *Appl. Phys. Lett.* **2009**, *94*, 071902.
(18) Abermann, R.; Koch, R. *Thin Solid Films* **1985**, *129*, 71.
(19) Leib, J.; Mönig, R.; Thompson, C. V. *Phys. Rev. Lett.* **2009**, *102*, 256101.
(20) Krevelen, D. W. V. *Properties of Polymers*; Elsevier: Amsterdam, The Netherlands, 1997.
(21) Schmid, H.; Wolf, H.; Allenspach, R.; Riel, H.; Karg, S.; Michel, B.; Delamarche, E. *Adv. Funct. Mater.* **2003**, *13* (2), 145.
(22) Thurner, G.; Abermann, R. *Thin Solid Films* **1990**, *192*, 277.
(23) Koch, R.; Abermann, R. *Thin Solid Films* **1986**, *140*, 217.
(24) Schneider, C. M.; Bressler, P.; Schuster, P.; Kirschner, J.; De Miguel, J. J.; Miranda, R. *Phys. Rev. Lett.* **1990**, *64*, 1059.
(25) Bodö, P.; Sundgren, J. E. *Thin Solid Films* **1986**, *136*, 147.
(26) Jo, B. H.; Lerberghe, L. M.; Motsegood, K. M.; Beebe, D. J. *J. Microelectromech. Syst.* **2000**, *9* (1), 76.

AM1002537